

Buckling Behaviour of Axially Loaded CFRP Reinforced Steel Cylinders

Toyohashi University of Technology
Toyohashi University of Technology
Toyohashi University of Technology

student member
Regular member

^oKrishna Kumar Bhetwal
Seishi Yamada, Yukihiro Matsumoto, Masayuki Yanagida
Sreng Sonit

1. Introduction

It is well-known that isotropic metal cylindrical shells under compression have buckling behaviour which is very sensitive to initial geometric imperfections¹⁾. In the case of orthotropic CFRP material, the angles and dispositions of fibre orientations, as well as the magnitudes of any imperfections, have been suggested to affect the buckling behaviour²⁾. In this paper, the buckling behaviour of axially loaded CFRP reinforced steel cylinders have been made clear through the fully nonlinear numerical experiments.

2. Method of Analysis

As shown in Fig. 1, the analytical model, having length L , radius of curvature R , shell thickness t , and axial load P is adopted here. The coordinate of shell is taken as x , y and z and the corresponding arbitrary displacement on the middle surface is adopted as u , v and w . The shell is considered simply supported and corresponding boundary condition is adopted as

$$w = 0, \quad \partial^2 w / \partial x^2 = 0, \quad \partial u / \partial x = 0, \quad v = 0 \quad \text{at } x = 0, L \quad (1)$$

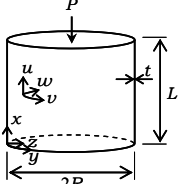


Fig. 1: Shell geometry

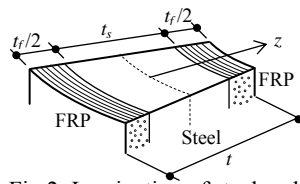


Fig. 2: Lamination of steel and FRP's

An anisotropic thin plate is considered and the material constants are obtained by using Halpin-Tsai equation³⁾ as

$$\begin{aligned} E_1 &= E_F V_F + E_P V_P \\ \mu_{12} &= \mu_F V_F + \mu_P V_P, \quad \mu_{21} = \frac{E_2}{E_1} \mu_{12} \\ E_2 &= \frac{1 + \xi \eta_2 V_F}{1 - \eta_2 V_F} E_P, \quad \eta_2 = \frac{E_F / E_P - 1}{E_F / E_P + \xi} \\ G_{12} &= \frac{1 + \xi \eta_{12} V_F}{1 - \eta_{12} V_F} G_P, \quad \eta_{12} = \frac{G_F / G_P - 1}{G_F / G_P + \xi} \end{aligned} \quad (2)$$

where, subscripts F and P denote fibre and polymer, V_F and V_P as volume fraction, E_1 as elastic coefficient and μ_{12} and μ_{21} as poison's ratios. E_2 is calculated by adopting parameter $\xi = 1 + 40 V_F^{10}$ and shell modulus G_{12} is obtained by adopting $\xi = 2$. In this study, expansion by the shear stiffness is neglected and stress and strain resultants for the laminated plates are obtained as

$$\begin{Bmatrix} n_x \\ n_y \\ n_{xy} \\ m_x \\ m_y \\ m_{xy} \end{Bmatrix} = \begin{bmatrix} A_{11} & A_{12} & 0 & B_{11} & B_{12} & 0 \\ A_{12} & A_{22} & 0 & B_{12} & B_{22} & 0 \\ 0 & 0 & A_{66} & 0 & 0 & B_{66} \\ B_{11} & B_{12} & 0 & D_{11} & D_{12} & 0 \\ B_{12} & B_{22} & 0 & D_{12} & D_{22} & 0 \\ 0 & 0 & B_{66} & 0 & 0 & D_{66} \end{bmatrix} \begin{Bmatrix} \varepsilon_x \\ \varepsilon_y \\ 2\varepsilon_{xy} \\ \kappa_x \\ \kappa_y \\ 2\kappa_{xy} \end{Bmatrix} \quad (3)$$

where (n_x, n_y, n_{xy}) are stress resultants, $(\varepsilon_x, \varepsilon_y, \varepsilon_{xy})$ are membrane strain, (m_x, m_y, m_{xy}) are moment resultants and, A_{ij} , B_{ij} and D_{ij} are membrane, membrane bending coupling and bending stiffnesses, respectively. For fully non-linear numerical experiments, linear sum of bi-harmonic function that satisfy the boundary condition of Eq.1 is adopted as the displacement functions u , v and w as shown in Eq. 4.

$$\begin{aligned} u &= \sum_{i=0,2,4,6}^J \sum_{j=1,3,5}^J u_{i,j} \cos(iy/R) \cos(j\pi x/L) \\ v &= \sum_{i=1,3,5}^J \sum_{j=0,2,4,6}^J v_{i,j} \sin(iy/R) \sin(j\pi x/L) \\ w &= \sum_{i=0,2,4,6}^J \sum_{j=1,3,5}^J w_{i,j} \cos(iy/R) \sin(j\pi x/L) \end{aligned} \quad (4)$$

where, $u_{i,j}$, $v_{i,j}$ and $w_{i,j}$ are the amplitudes of each harmonic function; i and j are the circumferential full-wave and the longitudinal half-wave number, respectively. The initial geometric imperfection is taken to consist of a harmonic

$$w^0 = w_{b,f}^0 \cos(by/R) \sin(f\pi x/L) \quad (5)$$

in which b and f represents the circumferential full-wave and longitudinal half-wave number, respectively. The sets of nonlinear algebraic equations characterizing the behaviour of the panels are obtained through the stationary of the TPE with respect to the each of the displacement degrees of freedom included in Eq.4. Solutions of these sets of nonlinear equations are achieved using a step-by-step process in which either load or displacements are used as control parameter. At each step, a Newton-Raphson iteration is used to provide convergence to an acceptable level of precision⁴⁾.

3. Results and Discussion

For the analysis of reinforced shells, the adopted geometrical parameters are $L/R = 0.512$, $R/t_s = 405$, $E_s = 205\text{GPa}$, $E_F = 235\text{GPa}$, $\mu_s = 0.3$, $\mu_F = 0.3$, $\mu_P = 0.34$. Fig.3 shows the results of numerical experiments of load-deflection curves in the case of circumferential full wave number $b=12$ having imperfection amplitude 0.8mm, 4.0mm and 4.8mm. The heavy solid lines denote the condition of no reinforcement. Similarly, the slight solid lines, broken lines and dotted lines denote for reinforcement $t_f = 4\text{mm}$ for angle of fibre orientation $\theta=0^\circ, 35^\circ, 90^\circ$, respectively. As shown in Fig. 3 the buckling capacity is high for reinforced condition at $\theta=90^\circ$ for all the amplitudes. Fig.4 shows the incremental displacement as the buckling modes in the case of the imperfection amplitude $w_{12,1}^0 = 0.8\text{mm}$ and 4.0mm. From this figure, it can be understood that the axial wavelength becomes longer when initial imperfection amplitude increases and there is little influence of reinforcement in the present numerical experimental models. Fig.5 shows the incremental deformation at the buckling load, for a typical case of these larger imperfections, exhibiting a mode, having

Key words: Cylindrical Shell, Buckling, RSM(Reduced Stiffness Method), CFRP(Carbon Fibre Reinforced Polymer)
DMV(Donnel-Mushtari-Vlasov), TPE(Total Potential Energy)
Contact: Toyohashi 441-8580, Toyohashi University of Technology, Tel: 0532-44-6849

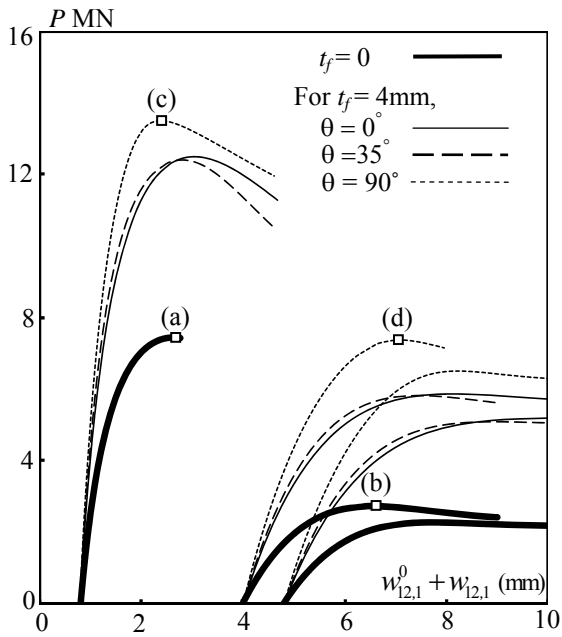
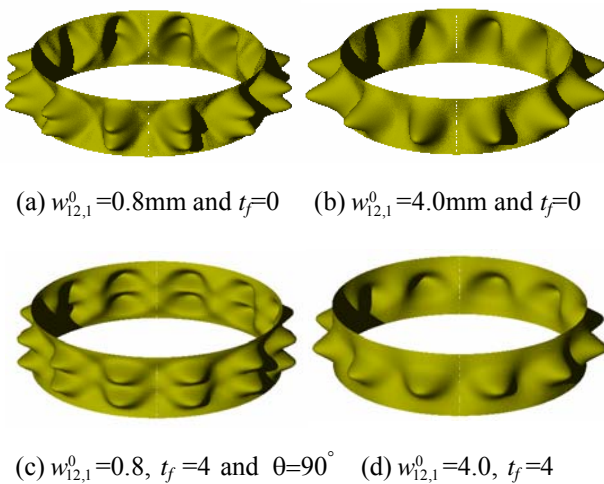
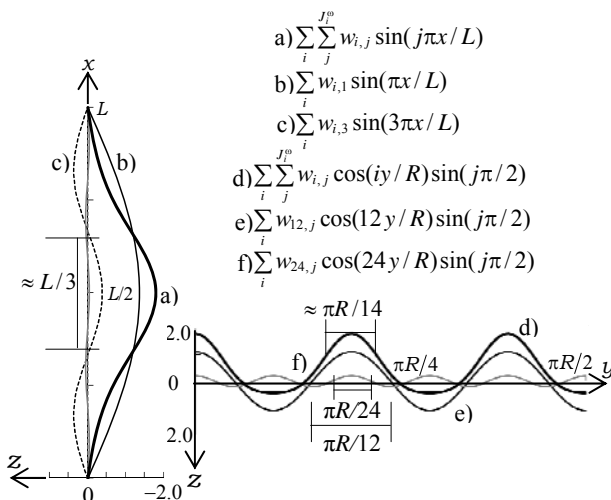
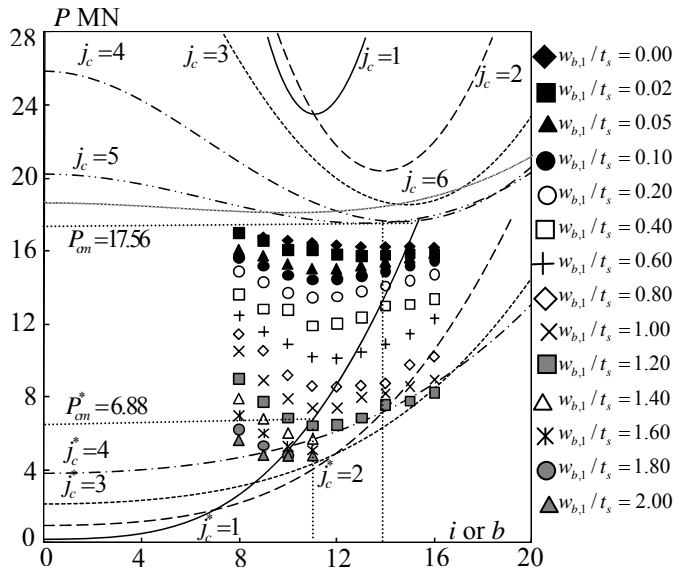


Fig. 3: Load-deflection curves

Fig. 4: incremental displacement for $t_s=4\text{mm}$ Fig. 5: Axially $y = 0$ and circumferential wave distributions at $x = L/2$ for $t_f = 4\text{mm}$, $\theta = 90^\circ$ and $w_{12,1}^0 = 4.0\text{mm}$

a circumferential wave number close to that predicted by the RSM with $t_f = 4$, $\theta = 90^\circ$, $b = 12$ and $f = 1$. A combination of $i = 12$ and 24 results in a compound circumferential mode shape as shown in Fig. 5, having a localized circumferential wavelength close to $i = 14$. Fig. 6 is the outcome of linear buckling analysis and RSM, obtained by using paper references 1) and 2). In Fig. 6, linear buckling loads are shown by upper spectrum of curves and RS buckling loads are shown by lower spectrum of curves. The linear buckling loads with varying longitudinal half-wave number j are defined as $P_{cm,j}$. Then, the corresponding circumferential full-wave number is obtained as $i_{cm}(j)$. After that, its RS critical load associated with $i_{cm}(j)$ is calculated as $P_{cm,j}^*$. As a result, the minimum value of $P_{cm,j}^*$ can be selected as the RS criterion. Also, in Fig. 6 the result of non-linear experiment is also plotted for axial wave number $b = 8 \sim 17.0$

Fig. 6: Load Spectra for $t_f=4\text{mm}$ and $\theta = 90^\circ$

4. Conclusion

The nonlinear numerical experiments have been carried out for CFRP laminated reinforced steel cylinders under axial compression and it is understood that depending upon the amplitude, buckling load carrying capacity differs. Also, from the nonlinear numerical experiment, it has shown that when initial imperfection amplitude increases, the axial wavelength becomes longer.

References

- 1) Yamada, S. and Croll J. G. A. (1999). "Contributions to understanding the behavior of axially compressed cylinders", Journal of Applied Mechanics, ASME, Vol. 66, 299-309.
- 2) Matsumoto, K., Yamada, S., Wang, H.T. and Croll, J.G.A. (2007). "Buckling and reduced stiffness criteria for FRP cylindrical shells under compression", Proceedings of Asia-Pacific Conference on FRP in Structures, IIFC, 465-470.
- 3) Jones, R. M. (1999). Mechanics of Composite Materials, 2nd Ed. Taylor & Francis.
- 4) Seishi Yamada, James G.A. Croll and Nobuhisa Yamamoto (2008) "Nonlinear Buckling of Compressed FRP Cylindrical Shells and Their Imperfection Sensitivity". Journal of Applied Mechanics, Vol. 75 / 041005-10, ASME